Published in final edited form as:
J Cell Sci. 2008 January 1; 121(0 1): . doi:10.1242/jcs.022681.

Phosphorylation of Vascular Endothelial Cadherin Controls Lymphocyte Emigration

Patric Turowski[1,9], **Roberta Martinelli**[1], **Rebecca Crawford**[1,6], **David Wateridge**[1,7], **Anna-Pia Papageorgiou**[1], **Maria Grazia Lampugnani**[2], **Alexander C. Gamp**[5], **Dietmar Vestweber**[5], **Peter Adamson**[1,8], **Elisabetta Dejana**[3,4], and **John Greenwood**[1,9]

[1]Division of Cell Biology, Institute of Ophthalmology, University College London, 11-43 Bath Street, London EC1V 9EL, UK

[2]Mario Negri Institute for Pharmacological Research, University of Milan, 20139 Milan, Italy

[3]IFOM-IEO Campus, Via Adamello 16, University of Milan, 20139 Milan, Italy

[4]Department of Biomolecular and Biotechnological Sciences, Faculty of Sciences, University of Milan, 20139 Milan, Italy

[5]Max-Planck-Institute of Molecular Biomedicine, Roentgenstr. 20, 48149 Muenster, Germany

Summary

Lymphocytes emigrate from the circulation to target tissues through the microvascular endothelial cell (EC) barrier. During paracellular transmigration cell-cell junctions have been proposed to disengage and provide homophilic and heterophilic interaction surfaces in a zip-like process. However, it is not known whether EC modulate junction proteins during this process. Here we show that tyrosine phosphorylation of adherens junction vascular endothelial cadherin (VEC) is required for successful transendothelial lymphocyte migration. We found that adhesion of lymphocytes or activation of the endothelial adhesion-receptor ICAM-1 led to tyrosine phosphorylation of VEC. Substitution of tyrosine to phenylalanine in VEC at position 645, 731 or 733 produced EC which were significantly less permissive to lymphocyte migration. We also found that these same tyrosines were involved in ICAM-1-dependent changes of VEC phosphorylation. ICAM-1 activation enhanced transendothelial permeability suggesting that junction disassembly occurred. In agreement the expression of Y645F, Y731F or Y733F VEC predominantly affected lymphocyte transmigration in paracellular areas. Taken together these results demonstrate that adherens junction phosphorylation constitutes a molecular endpoint of lymphocyte-induced vascular EC signaling and may be exploited as a new target of anti-inflammatory therapies.

Keywords

Lymphocyte Migration; VE-cadherin; Tyrosine Phosphorylation; Brain Endothelium; ICAM-1

[9]To whom correspondence should be addressed: p.turowski@ucl.ac.uk, Tel.: +44 207 608 6970, Fax.: +44 207 608 6810, j.greenwood@ucl.ac.uk, Tel.: +44 207 608 6858, Fax.: +44 207 608 6810.
[6]Present address: Kennedy Institute of Rheumatology, Imperial College, London W6 8LH, UK
[7]Present address: Faculty of Life Sciences, University of Manchester, UK
[8]Present address: Ophthaltec Limited, London SW1Y 4QU, UK

Europe PMC Funders Author Manuscripts

Introduction

Intercellular Adhesion Molecule-1 (ICAM-1) on the luminal surface membrane of vascular ECs plays a critical role during the egress of lymphocytes from the vascular compartment. It binds to β2 integrins such as LFA-1 (αL/β2, CD11a/CD18) on lymphocytes and promotes stable arrest (Butcher, 1991). However, endothelial ICAM-1 is not only a docking receptor for lymphocyte adhesion and migration but its engagement also triggers endothelial signaling cascades that contribute fundamentally to vascular compliance to lymphocyte diapedesis and the endothelial inflammatory response (Turowski et al., 2005). ICAM-1-induced signaling comprises changes in intracellular calcium and dynamic actin as well as the activation of the small GTPase rho, src and C protein kinases. Despite an increasing number of key players involved in ICAM-1-mediated endothelial signaling being identified, downstream effectors and molecular endpoints that ultimately modulate lymphocyte migration remain elusive.

Both tight and adherens junction (AJ) proteins form attachments between ECs and are major sites of regulating the transport of molecules and cells across vascular barriers (Bazzoni and Dejana, 2004). At least in the case of paracellular leukocyte extravasation various junction molecules disengage and in turn form homo- and heterophilic interactions with leukocyte adhesion proteins (Imhof and Aurrand-Lions, 2004; Muller, 2003; Rao et al., 2007). In this process the EC has been ascribed a rather passive role where junctions are forced open by the migrating leukocyte (Imhof and Aurrand-Lions, 2004; Shaw et al., 2001). We investigated whether intercellular junction modulation was part of the endothelial response to lymphocyte migration.

Results and Discussion

Migration of antigen-activated lymphocytes across brain microvascular ECs in vitro does not require inflammatory cytokine stimulation, occurs in the absence of chemokine gradients and is predominantly dependent on ICAM-1 but not VCAM-1 (Greenwood et al., 1995). ICAM-1-mediated signaling pathways involve rho GTPases and MAP kinase cascades and have generally been studied by antibody-mediated crosslinking of serum-starved cells (Turowski et al., 2005). In rat brain microvascular ECs (GPNT) ICAM-1 activation led to a rapid and transient increase of tyrosine phosphorylation of a number of proteins which was maximal within 10-15 minutes of ICAM-1 stimulation (Fig 1 A). When analysed by immunocytochemistry (Fig. 1 B) the increase in phospho-tyrosine was most marked at the intercellular junction area and preceded major actin re-arrangements typically seen following ICAM-1 crosslinking (Adamson et al., 1999). Immunoprecipitation and subsequent phospho-tyrosine analysis of junction proteins revealed that VEC (Fig. 1 C, E), but not ZO-1, occludin, or any of the catenins (Fig. 2), displayed altered tyrosine phosphorylation following ICAM-1 crosslinking. Phosphorylation of VEC was rapid and transient, reaching a maximum after 15 minutes of ICAM-1 crosslinking (Fig. 1 D). It depended on upstream signaling by rho GTPase, dynamic actin and also intracellular Ca2+ (Fig. 1 H), all of which are essential for successful lymphocyte migration (Turowski et al., 2005). No involvement of src family protein kinases was observed in our experimental set up. This is in contrast to a recent report by Allingham et al. (2007) and may reflect that different signaling modules are activated and utilized by different subsets of EC and/or leukocytes. Significantly, T cell adhesion to GPNT cells also induced a significant rise in VEC tyrosine phosphorylation (Fig 1. F, G), albeit with a slightly delayed time course (presumably reflecting settling and adhesion times). Taken together these data suggested that interendothelial junctions could be molecular endpoints of ICAM-1-mediated signaling during leukocyte adhesion and migration.

To study the functional significance of ICAM-1-mediated VEC phosphorylation, the structure of the cytoplasmic domain of VEC was further analysed in silico and by mutagenesis. The cytoplasmic tail of VEC contains 8 conserved tyrosine residues (Fig. 3 A), three of which are predicted to constitute phospho-acceptor sites for insulin receptor family (Y645, Y731) or src family (Y685) protein kinases (http://kinasephos.mbc.nctu.edu.tw, data not shown). A structural computer model of the VEC intracellular domain bound to β-catenin suggested that Y725, Y731 and Y733 were exposed and accessible to phosphorylation whilst Y685, Y757 and Y774 were oriented towards the bound β-catenin and possibly inaccessible (Fig. 3 B). Y645 and Y658 are located outside of this area in a domain predicted to mediate p120 binding (Lampugnani et al., 2002).

Recently, Y658, Y685 and Y731 have been described as target phosphorylation sites (Potter et al., 2005; Wallez et al., 2006) and we therefore addressed whether phosphorylation of any of these three tyrosines residues was important for lymphocyte migration. For this we have derived EC lines from VEC-null mouse endotheliomas that re-expressed wt, Y658F, Y685F or Y731F VEC. VEC expression levels and localization were similar in all four cell lines (Fig. 4 A, B), suggesting that Y to F mutations did not interfere with junctional targeting. Migration of activated T cells across VEC-null EC was very low but significantly enhanced when wt VEC was re-expressed (Fig. 4 C). A similar, ca. two-fold increase was observed when either a clonal cell line stably re-expressing wt VEC or a pool of cells transiently expressing EGFP –VEC was analysed. Absolute migration rates measured after 4 hours of lymphocyte co-culture increased from ca. 10 % to 20-25 % when VEC was reconstituted in null endothelioma cells and were then in the same range than what is usually observed across GPNT brain mivcrovascular EC (ca. 30 %) indicating that the expression of VEC is vital to the functional integrity of the vascular endothelium. This was somewhat unexpected since VEC disruption using antibodies has been reported to enhance neutrophil migration in vivo (Gotsch et al., 1997). However, VEC elimination leads to significant changes in the AJ composition (Zanetta et al., 2005) and may in this way inhibit leukocyte migration indirectly. Alternatively, VEC may have opposing effects on the migration of lymphocytes and neutrophils. When cells expressing mutants of VEC were analysed we found that the re-expression of VEC carrying single mutations in Y658 or Y685 did not have any effect on lymphocyte transmigration (Fig. 4 D). However, mutation of Y731 led to a ca. two-fold reduction in lymphocyte migration. This indicated that VEC phosphorylation may be important for leukocyte migration.

To test the role of intracellular tyrosines of VEC more systematically and in an EC system more relevant to inflammation, VEC containing single Y to F substitutions was transiently expressed as amino-terminal fusions of EGFP in GPNT brain microvascular ECs. Expression levels and overall localization of the individual VEC mutants were similar and mostly restricted to the periphery of the cell (Fig 5 A). Some cells expressed the protein at very high levels throughout the cell but these appeared non-viable and were never integrated into endothelial monolayers. In all other expressing cells, EGFP was almost exclusively found at cell-cell junctions once EC monolayers were formed (Fig. 5 B). Again we observed that the introduction of Y731F VEC significantly reduced lymphocyte migration. In addition we also observed impaired lymphocyte migration across GPNT expressing Y645F or Y733F VEC (Fig. 5 C). By contrast, the introduction of wt VEC or any other Y to F mutant did not affect migration. The inhibitory effect of Y645F and Y733F VEC was also corroborated in a VEC-null background. Transient expression of Y645F or Y733F but not any other VEC-GFP mutants, produced endothelioma cells with a similar propensity to reduced lymphocyte migration (Fig 5 D). In all cases the mutant VEC clearly interfered on the level of lymphocyte diapedesis since adhesion rates were comparable.

Commercially available antibodies against VEC phosphorylated at Y658 or Y731 (Potter et al., 2005) were not reactive with VEC immunoprecipitates from ICAM-1 crosslinked cells (data not shown) and recognized the same protein in whole cell lysates whether full length or truncated VEC (Lampugnani et al., 2002) was expressed (data not shown). To examine whether ICAM-1-induced tyrosine phosphorylation involved the Y at positions 645, 731 or 733 the phosphorylation of wt and mutant GFP-VEC was analysed in CHO-ICAM-1 cells. Crosslinking of ectopic human ICAM-1 on CHO cells induced tyrosine phosphorylation of co-expressed GFP-VEC in a time dependent manner (Fig. 6 A), similar to that observed in GPNT cells. When the phosphorylation status of the Y to F mutants of GPF-VEC was tested, only Y733F displayed significantly reduced tyrosine phosphorylation in response to ICAM-1 ligation (Fig. 6 B), suggesting that this mutation interfered with tyrosine phosphorylation of VEC. Next, GFP-VEC was also analysed from 32P-labelled cells. Significantly, GFP-VEC was immunoprecipitated as a strongly phosphorylated protein, with the majority of phosphate present as phospho-serine and only very little phospho-tyrosine (data not shown). This observation is also in agreement with the recently reported phosphorylation of S665 by PAK (Gavard and Gutkind, 2006). Tryptic phospho-peptide mapping revealed at least five groups of peptides with apparently variable phosphorylation levels (Fig. 6 C, D; Fig. S2). When ICAM-1 was crosslinked most phospho-peptides remained unchanged but two peptides displayed significantly reduced chromatographic mobility, indicative of additional phosphorylation (arrowed in panel D). The Y645F mutation suppressed phosphorylation of one peptide but enhanced that of the other indicating that this mutation may interfer with phosphorylation site recognition. Y731F induced a perfect reversal to VEC from non-crosslinked cells suggesting that this site was directly phosphorylated. Overall phosphorylation was low in Y733F and the migration of most phospho-peptide was altered which suggested that this mutation rendered most sites unphosphorylatable. More refined phospho-peptide analysis by mass spectroscopy will be required to delineate the exact phosphorylation changes that occur on tyrosines and serines when EC are stimulated. In summary, VEC mutations of tyrosines at position 645, 731 or 733, which dominantly inhibited lymphocyte migration, also affected ICAM-1-mediated VEC phosphorylation and this suggested that these events were mechanistically linked. VEC has been reported to be phosphorylated on tyrosine under various conditions (Andriopoulou et al., 1999; Esser et al., 1998) and indeed we found that tyrosine phosphorylation was also increased when GPNT cells were treated with a variety vasoactive compounds (Fig. 7 A). Generally it is thought that such phosphorylation induces the disruption of AJs which can be measured by concomitant rises in transendothelial permeability. We found that ICAM-1 crosslinking is likely to affect AJ organization since it also induced an increase in paracellular permeability (Fig. 7 B) and monolayer impedance (data not shown). However, in contrast to growth factor stimulation where this is frequently associated with altered catenin binding (Lampugnani et al., 1997; Potter et al., 2005; Weis et al., 2004), ICAM-1 ligation did not affect the levels of VEC-associated α-, β-, or γ- catenin (Fig. 7 C, D), suggesting that the molecular mechanism may be different. Intuitively, ICAM-1-mediated VEC phosphorylation may lead to the disengagement of AJs and thus facilitate the path during paracellular migration. In support of such a mechanism we found that the expression of Y645F, Y731F or Y733F VEC led to a significant reduction of migration in paracellular areas of the EC monolayer (Fig. 7 E) and this correlated well with the general rate of inhibition (see Fig. 5 C). Therefore paracellular but not transcellular migration may be affected by dysfunctional VEC. However, more careful dynamic confocal microscopy of stable transfectants would be required to draw a definite conclusion, in particular since transcellular migration also relies on juxta-junctional positioning of the lymphocyte and subsequently on a transcytotic pathway (Carman et al., 2007; Millan et al., 2006), in which VEC may also be involved (Gavard and Gutkind, 2006; Xiao et al., 2005).

Leukocyte adhesion and subsequent ICAM-1 engagement on EC induces an endothelial response and a complex network of signaling pathways which regulate the inflammatory response of the endothelium (Turowski et al., 2005). From the results presented here, tyrosine phosphorylation of VEC meets all the criteria for a molecular endpoint of an endothelial signaling cascade that regulates lymphocyte migration: It is induced by surface engagement of ICAM-1, it can be placed down-stream of pathways that have previously been identified to affect lymphocyte migration, and it appears to regulate paracellular migration directly. The importance of this mechanism and its general validity is underscored by recent findings by Allingham et al. (2007) who reported similar VEC phosphorylation to operate when neutrophils migrate across HUVEC. Collectively, these results demonstrate that VEC plays a more active role during leukocyte migration than previously anticipated. Single amino acid mutations, namely at Y645, Y731 or Y733, suppressed this function and surprisingly did so in a dominant fashion. Since dominant effects are rarely observed with mutations introducing non-phosphorylatable amino acid (as opposed to phospho-mimetic substitutions), it will be interesting to elucidate how these mutations interfere with the function of endogenous VEC during leukocyte migration. Currently, anti-adhesion therapies are amongst the most specific and advanced strategies to treat inflammation. The identification of a dominant molecular endpoint of adhesion-induced signaling may constitute a valid target for novel anti-inflammatory therapies.

Material and Methods

Cell Culture And Treatment

The SV40 large T-immortalized rat brain microvascular EC line GPNT (Romero et al., 2003) and middle T transformed mouse brain endothelioma cells bEND5 (Lyck et al., 2003) were grown as previously described. Mouse EC with a homozygous null mutation of the VEC gene and the cell line re-expressing wild-type VEC derived by retroviral gene transfer have been described in detail (Lampugnani et al., 2002). Additionally, cell lines that stably express Y658F, Y685F or Y731F VEC have been generated in the same manner. Wild-type Chinese hamster ovary (CHO) cells and stable transfectants expressing human ICAM-1 (a kind gift by Prof. Jeremy Pearson, King’s College London, UK) were cultured in DMEM/F12 supplemented with 10 % FCS.

Antibody-mediated ICAM-1 cross-linking was performed as previously described in serum starved cells (Adamson et al., 1999) using monoclonal antibodies against rat (clone 1A29), mouse (clones YNI-1 and 25ZC7) or human (clone 15.2) ICAM-1.

Lymphocyte co-cultures with ECs was performed with peripheral lymph node cells (PLNCs) isolated from Lewis rats (Harlan Olac) as previously described (Adamson et al., 1999). For biochemical analysis of the EC, PLNCs were washed and fixed using 3.7 % formaldehyde before being added to EC, thus avoiding analysis of lymphocyte proteins after cell lysis. For adhesion assays, PLNCs were fluorescently labeled with 1 μM calcein-AM (Molecular Probes) before addition to EC monolayers (ca. 10 labeled PLNCs/EC). Co-cultures were left at 37°C for 60 minutes and adherent T cells quantified in a fluorescent plate reader. Migration assays were performed using a myelin basic protein (MBP) Ag-specific T cell line by time-lapsed video microscopy as previously reported (Adamson et al., 1999). Migration was considered paracellular when it clearly occurred in the phase bright area that defined the periphery of the EC. Only T cells that completed transmigration were counted as migrated.

Permeability assays on GPNT cells were conducted in transwell inserts using FITC-dextrans (Sigma) of varying molecular weight (1 mg/ml) (Esser et al., 1998).

Cell lysis, immunoprecipitations and western blots

Total cell extracts were prepared in 50 mM Tris/Cl pH 7.5, 1 % SDS, 1 mM orthovanadate. For immunoprecipitations cells were lysed in a buffer containing 10 mM Hepes/NaOH pH 7.4, 100 mM NaCL, 50 mM β-glycerophosphate, 2 mM $MgCl_2$, 5 mM EGTA, 5 mM EDTA, 1 % Igepal (Sigma), 1 mM orthovanadate, 1 mM NaF and protease inhibitors (Roche). Clarified cell extracts were incubated with 1 μg of anti-VEC (Santa Cruz, 6458), anti-α- or -β-catenin (Sigma), γ-or p120 catenin (BD Biosciences) or 5 μg of anti-GFP antibody (Abcam 290). Antigen-antibody complexes were collected using protein A- or G-sepharose beads (GE Healthcare). SDS-PAGE and immunoblotting was performed as previously described (Turowski et al., 1999) using anti-phosphotyrosine (4G10, PY20 or RC20H), anti-VEC or anti-catenin. For quantitative analyses immunoblots were scanned and quantified using the NIH imaging software ImageJ. The intensity of the phospho-tyrosine signals was normalized to the corresponding amount of VEC, and expressed as fold-increase of untreated controls.

Immunofluorescence

GPNT cells were fixed in 3.7% formaldehyde and extracted with acetone (−20°C). For the detection of phospho-tyrosine the monoclonal antibody 4G10 (Upstate) was biotinylated and used at 2 μg/ml. Cells were then stained using streptavidin-texas red (GE Healthcare) and phalloidin-oregon green (Molecular Probes; 1:50). VEC was revealed using a polyclonal goat antibody (sc-6458, Santa Cruz). Cells were mounted using Moviol 4-88 and analyzed by standard epifluorescent or confocal microscopy (Turowski et al., 1999).

Plasmids, mutagenesis and transfections

Mouse VEC was mutagenised using the Quickchange mutatgenesis (Stratagene). Subsequently, wt and mutant VEC were cloned into pEGFP-N1 (BD Biosciences) to result in expression of the open reading frame of mouse VEC (aa 1- 784), followed by the linker sequence LVDPPVAT and the entire sequence of EGFP. Plasmids were verified by DNA sequencing and purified using endotoxin-free preparation methods (Qiagen). Subsequently, GPNT or mouse VEC-null endothelioma cells were nucleofected using 20 μg plasmid per 2-3 × 10^6 cells according to the manufacturer's instructions (Amaxa). CHO-ICAM-1 cells were transfected using lipofectamine 2000 (Invitrogene).

32P labeling and phosphoamino acid and –peptide analysis

Transfected CHO-ICAM-1 cells were labeled with phosphorus-32 (PBS 13; GE Healthcare; 20 MBq/ml) in phosphate-free DMEM for 3 h, ICAM-1 crosslinked, lysed and VEC-GFP precipitated using 5 μg of a polyclonal anti-GFP antibody (Abcam 290). Immunoprecipitates were resolved by SDS-PAGE and transferred to nitrocellulose or PVDF. Radiolabelled VEC was excised and subjected to acid hydrolysis for phosphoamino acid analysis or to digestion with trypsin using standard procedures (Boyle et al., 1991). Amino acids or phosphopeptides were subsequently resolved on cellulose TLC plates by electrophoresis and chromatography and detected by autoradiography.

Computer model of the VEC cytoplasmic domain

A homology-based model was obtained using the coordinates of E-cadherin-β-catenin complex (pdb: 1i7x, 1i7w). Cytoplamic domains of VEC from various species and E-cadherin were aligned using ClustalW (www.ebi.ac.uk/clustalw/). The optimal alignment was used by PyMol (http://pymol.sourceforge.net/) to build the VEC model.

Acknowledgments

We thank David Barford for help with deriving the structure model of the VEC-β-catenin complex. This work was supported by a Programme Grant from the Wellcome Trust (062403, awarded to J.G. and P.A.) and in part by the European Community (NoE MAIN 502935, to E.D.).

References

Adamson P, Etienne S, Couraud PO, Calder V, Greenwood J. Lymphocyte migration through brain endothelial cell monolayers involves signaling through endothelial ICAM-1 via a rho-dependent pathway. J. Immunol. 1999; 162:2964–2973. [PubMed: 10072547]

Allingham MJ, van Buul JD, Burridge K. ICAM-1-Mediated, Src- and Pyk2-Dependent Vascular Endothelial Cadherin Tyrosine Phosphorylation Is Required for Leukocyte Transendothelial Migration. J. Immunol. 2007; 179:4053–4064. [PubMed: 17785844]

Andriopoulou P, Navarro P, Zanetti A, Lampugnani MG, Dejana E. Histamine induces tyrosine phosphorylation of endothelial cell-to-cell adherens junctions. Arterioscler. Thromb. Vasc. Biol. 1999; 19:2286–2297. [PubMed: 10521356]

Bazzoni G, Dejana E. Endothelial cell-to-cell junctions: molecular organization and role in vascular homeostasis. Physiol Rev. 2004; 84:869–901. [PubMed: 15269339]

Boyle WJ, van der GP, Hunter T. Phosphopeptide mapping and phosphoamino acid analysis by two-dimensional separation on thin-layer cellulose plates. Methods Enzymol. 1991; 201:110–149. [PubMed: 1943760]

Butcher EC. Leukocyte-endothelial cell recognition: three (or more) steps to specificity and diversity. Cell. 1991; 67:1033–1036. [PubMed: 1760836]

Carman CV, Sage PT, Sciuto TE, de la Fuente MA, Geha RS, Ochs HD, Dvorak HF, Dvorak AM, Springer TA. Transcellular diapedesis is initiated by invasive podosomes. Immunity. 2007; 26:784–797. [PubMed: 17570692]

Durieu-Trautmann O, Chaverot N, Cazaubon S, Strosberg AD, Couraud PO. Intercellular adhesion molecule 1 activation induces tyrosine phosphorylation of the cytoskeleton-associated protein cortactin in brain microvessel endothelial cells. J. Biol. Chem. 1994; 269:12536–12540. [PubMed: 7909803]

Esser S, Lampugnani MG, Corada M, Dejana E, Risau W. Vascular endothelial growth factor induces VE-cadherin tyrosine phosphorylation in endothelial cells. J. Cell Sci. 1998; 111(Pt 13):1853–1865. [PubMed: 9625748]

Gavard J, Gutkind JS. VEGF controls endothelial-cell permeability by promoting the beta-arrestin-dependent endocytosis of VE-cadherin. Nat. Cell Biol. 2006; 8:1223–1234. [PubMed: 17060906]

Gotsch U, Borges E, Bosse R, Boggemeyer E, Simon M, Mossmann H, Vestweber D. VE-cadherin antibody accelerates neutrophil recruitment in vivo. J. Cell Sci. 1997; 110(Pt 5):583–588. [PubMed: 9092940]

Greenwood J, Wang Y, Calder VL. Lymphocyte adhesion and transendothelial migration in the central nervous system: the role of LFA-1, ICAM-1, VLA-4 and VCAM-1. off. Immunology. 1995; 86:408–415. [PubMed: 8550078]

Huber AH, Weis WI. The structure of the beta-catenin/E-cadherin complex and the molecular basis of diverse ligand recognition by beta-catenin. Cell. 2001; 105:391–402. [PubMed: 11348595]

Huber D, Balda MS, Matter K. Occludin modulates transepithelial migration of neutrophils. J. Biol. Chem. 2000; 275:5773–5778. [PubMed: 10681565]

Imhof BA, Aurrand-Lions M. Adhesion mechanisms regulating the migration of monocytes. Nat. Rev. Immunol. 2004; 4:432–444. [PubMed: 15173832]

Lampugnani MG, Corada M, Andriopoulou P, Esser S, Risau W, Dejana E. Cell confluence regulates tyrosine phosphorylation of adherens junction components in endothelial cells. J. Cell Sci. 1997; 110(Pt 17):2065–2077. [PubMed: 9378757]

Lampugnani MG, Zanetti A, Breviario F, Balconi G, Orsenigo F, Corada M, Spagnuolo R, Betson M, Braga V, Dejana E. VE-cadherin regulates endothelial actin activating Rac and increasing membrane association of Tiam. Mol. Biol. Cell. 2002; 13:1175–1189. [PubMed: 11950930]

Lyck R, Reiss Y, Gerwin N, Greenwood J, Adamson P, Engelhardt B. T-cell interaction with ICAM-1/ICAM-2 double-deficient brain endothelium in vitro: the cytoplasmic tail of endothelial ICAM-1 is necessary for transendothelial migration of T cells. Blood. 2003; 102:3675–3683. [PubMed: 12893765]

Millan J, Hewlett L, Glyn M, Toomre D, Clark P, Ridley AJ. Lymphocyte transcellular migration occurs through recruitment of endothelial ICAM-1 to caveola- and F-actin-rich domains. Nat. Cell Biol. 2006; 8:113–123. [PubMed: 16429128]

Muller WA. Leukocyte-endothelial-cell interactions in leukocyte transmigration and the inflammatory response. Trends Immunol. 2003; 24:327–334. [PubMed: 12810109]

Potter MD, Barbero S, Cheresh DA. Tyrosine phosphorylation of VE-cadherin prevents binding of p120- and beta-catenin and maintains the cellular mesenchymal state. J. Biol. Chem. 2005; 280:31906–31912. [PubMed: 16027153]

Rao RM, Yang L, Garcia-Cardena G, Luscinskas FW. Endothelial-dependent mechanisms of leukocyte recruitment to the vascular wall. Circ. Res. 2007; 101:234–247. [PubMed: 17673684]

Romero IA, Radewicz K, Jubin E, Michel CC, Greenwood J, Couraud PO, Adamson P. Changes in cytoskeletal and tight junctional proteins correlate with decreased permeability induced by dexamethasone in cultured rat brain endothelial cells. Neurosci. Lett. 2003; 344:112–116. [PubMed: 12782340]

Shaw SK, Bamba PS, Perkins BN, Luscinskas FW. Real-time imaging of vascular endothelial-cadherin during leukocyte transmigration across endothelium. J. Immunol. 2001; 167:2323–2330. [PubMed: 11490021]

Turowski P, Adamson P, Greenwood J. Pharmacological targeting of ICAM-1 signaling in brain endothelial cells: potential for treating neuroinflammation. Cell Mol. Neurobiol. 2005; 25:153–170. [PubMed: 15962512]

Turowski P, Myles T, Hemmings BA, Fernandez A, Lamb NJC. Vimentin dephosphorylation by protein phosphatase 2A is modulated by the targeting subunit B55. Mol. Biol. Cell. 1999; 10:1997–2015. [PubMed: 10359611]

Wallez Y, Cand F, Cruzalegui F, Wernstedt C, Souchelnytskyi S, Vilgrain I, Huber P. Src kinase phosphorylates vascular endothelial-cadherin in response to vascular endothelial growth factor: identification of tyrosine 685 as the unique target site. Oncogene. 2006

Weis S, Cui J, Barnes L, Cheresh D. Endothelial barrier disruption by VEGF-mediated Src activity potentiates tumor cell extravasation and metastasis. J. Cell Biol. 2004; 167:223–229. [PubMed: 15504909]

Xiao K, Garner J, Buckley KM, Vincent PA, Chiasson CM, Dejana E, Faundez V, Kowalczyk AP. p120-Catenin regulates clathrin-dependent endocytosis of VE-cadherin. Mol. Biol. Cell. 2005; 16:5141–5151. [PubMed: 16120645]

Zanetta L, Corada M, Grazia LM, Zanetti A, Breviario F, Moons L, Carmeliet P, Pepper MS, Dejana E. Downregulation of vascular endothelial-cadherin expression is associated with an increase in vascular tumor growth and hemorrhagic complications. Thromb. Haemost. 2005; 93:1041–1046. [PubMed: 15968386]

Europe PMC Funders Author Manuscripts

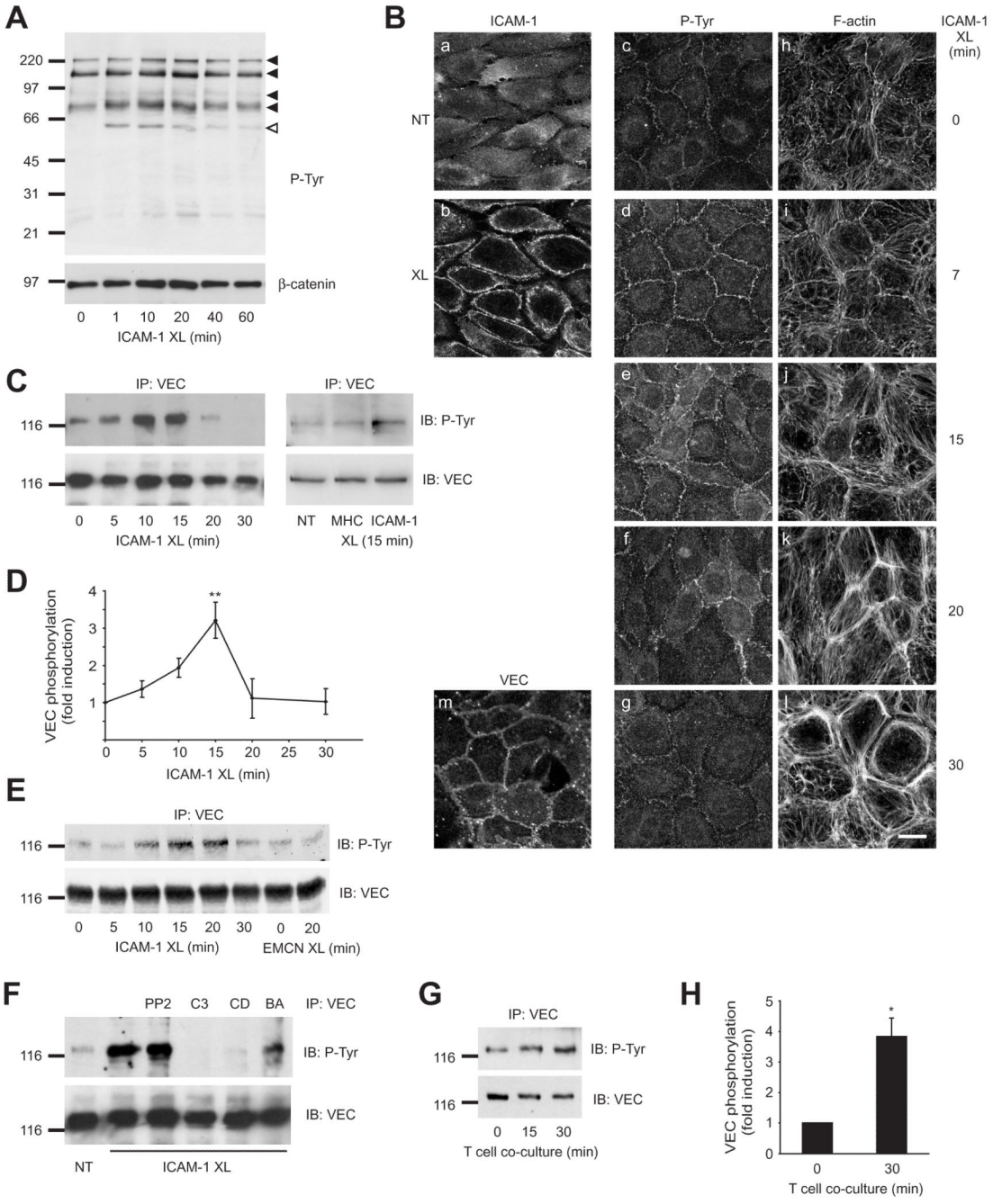

Fig. 1.

Tyrosine phosphorylation of VEC following ICAM-1 cross-linking or adhesion of lymphocytes. (A) GPNT brain microvascular ECs were grown to confluence, serum starved and ICAM-1 crosslinked (XL) for the indicated times. Total protein extracts (ca. 50 μg) were analyzed by immunoblotting with anti-phospho-tyrosine antibodies. Blots were subsequently stripped and probed for β-catenin as loading control. Four proteins with apparent molecular masses of 220, 140, 94 and 83 kDa (previously identified as cortactin (Durieu-Trautmann et al., 1994)) displayed clearly enhanced tyrosine phosphorylation and are indicated by filled arrowheads. Open arrowheads indicate the position of the IgG heavy chains of the crosslinking antibody. (B) Confluent GPNT brain microvascular ECs were

serum starved and either left untreated (a, m) or ICAM-1 cross-linked for 15 minutes (b) or the indicated times (c-l). Cells were fixed, extracted and stained for surface ICAM-1 (a, b), phospho-tyrosine (c-g), F-actin (h-l) or VEC (m). Bar, 10 μm. (C-F) Confluent GPNT cells (C, D, F) or mouse brain endothelioma EC, bEND5 (E), were serum starved and subjected to crosslinking of ICAM-1 (XL) or unrelated surface molecules (MHC class I, EMCN: endomucin). At the indicated times cells were washed and lysed. VEC immunoprecipitates were then analysed by immunoblotting using either anti-phospho-tyrosine or –VEC antibodies. (D) The amount of tyrosine-phosphorylated VEC (in panel C) was quantified by densitometry from five independent experiments and expressed as fold-increase of untreated controls (means ± SEM). (F) Prior to ICAM-1 crosslinking (15 minutes) and where indicated, cells were pre-treated using PP2 (10 μM, 30 minutes), C3 transferase (2 μg/mL, 16 hours), cytochalasin D (CD, 2 μM, 30 minutes) or BAPTAM (BA, 20 μM, 30 minutes). (G, H) Confluent GPNT were co-cultured with 2×10^6 /ml rat peripheral lymph node (PLN) lymphocytes (ca. 5 lymphocytes per EC). At the indicated times cells were lysed and VEC immunoprecipitates prepared and analysed as described above. (H) Data from four independent experiments were quantified by densitometry, normalized and expressed as fold-increase of untreated controls (means ± SEM). Significant differences were determined by Student's *t* test, * $p<0.003$, ** $p<0.002$. In all blots the position of size markers (in kDa) is indicated on the left.

Europe PMC Funders Author Manuscripts

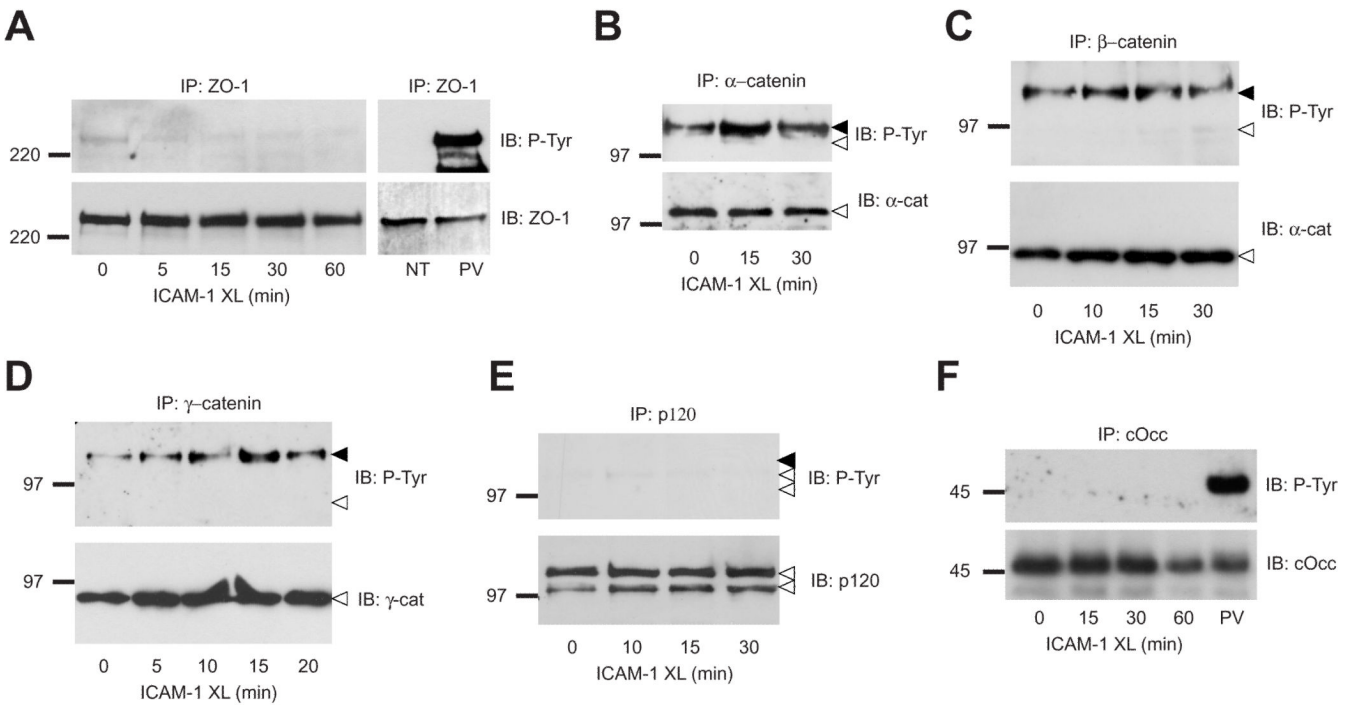

Fig. 2.

Analysis of tyrosine phosphorylation of other junction proteins in ICAM-1 stimulated ECs. (A-E) Confluent GPNT cells were serum starved and ICAM-1 crosslinked (XL). At the indicated times cells were washed, lysed and subjected to immunoprecipitation of ZO-1 (A) and catenins as indicated (B-E). Immunoprecipitates were then analysed by immunoblotting using either anti-phospho-tyrosine, –ZO-1, -VEC or -catenin antibodies. Black and white arrowheads in panels A-E indicate the position of migration of VEC and relevant catenins, respectively, as determined by stripping and re-probing of the immunoblots. P120 immunoprecipitates did not contain detectable VEC, whether phosphorylated (black arrowhead) or not (data not shown). (F) The chicken occludin-expressing GPNT cell line (see Supplemental Fig. S1) was grown to confluence, serum starved and ICAM-1 crosslinked (XL). At the indicated times chicken occludin was immunoprecipitated and analysed by immunoblotting for phospho-tyrosine or occludin. In all blots the position of size markers (in kDa) is indicated on the left.

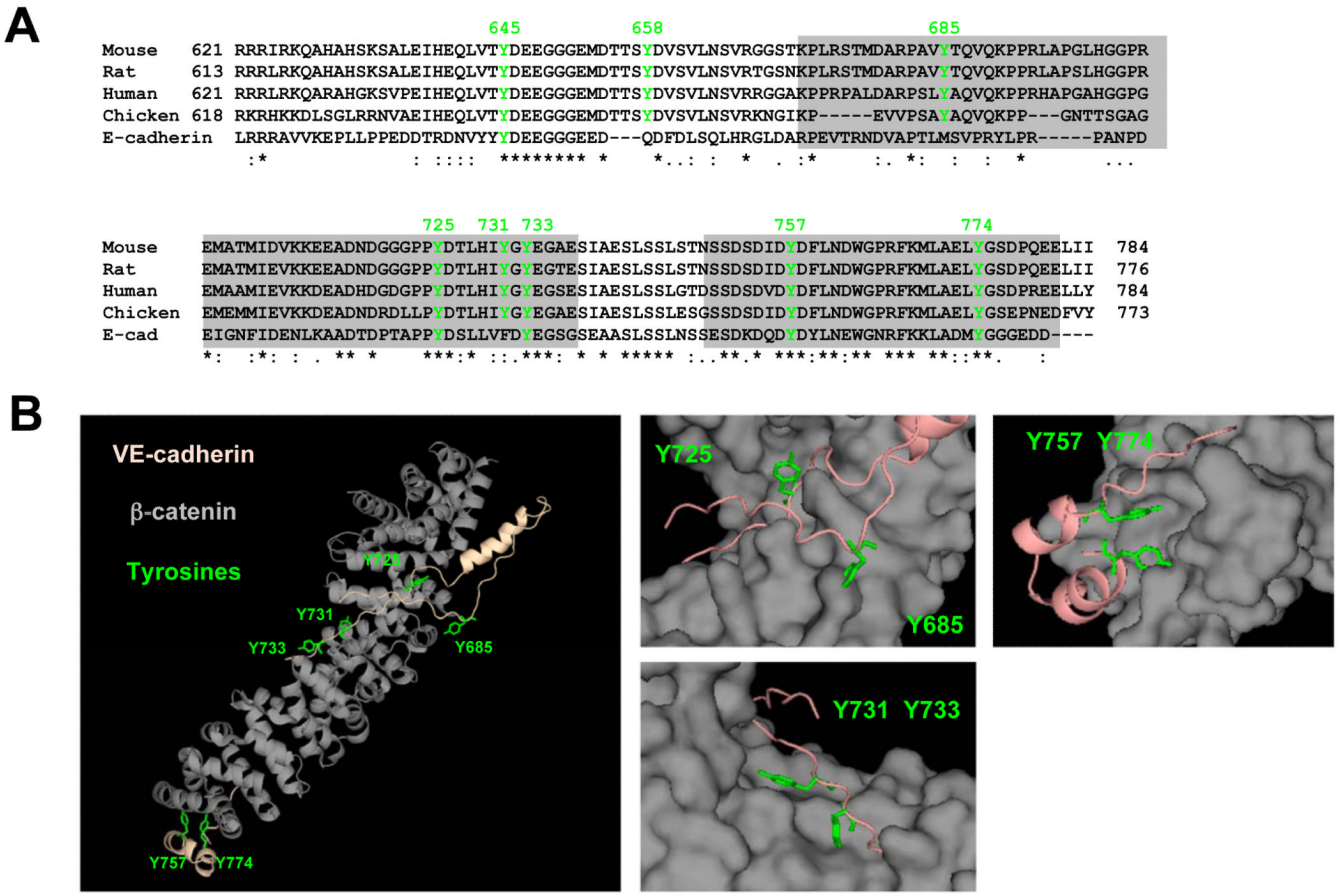

Fig. 3.

Conserved tyrosines in the cytoplasmic domain of VEC. (A) Sequence alignment of cytoplasmic domains of VEC and mouse E-cadherin. Tyrosines conserved in VEC and their relative position (mouse/human) are indicated in green. Identical residues, conserved and semi-conserved substitutions are indicated by asterisks, colons and dots, respectively. Grey boxes denote areas corresponding to those parts of E-cadherin which interact with β-catenin in co-crystals (Huber and Weis, 2001). (B) Mouse VEC was computer-modeled on the crystal structure of mouse E-cadherin in the E-cadherin-β-catenin complex (i.e. boxed in panel A) (pdb: 1i7x, 1i7w). Shown in the left panel is a ribbon representation of this model with the position and orientation of six tyrosines highlighted in green. The right panels represent enlarged views of areas surrounding these tyrosines. The β-catenin chain is in a space filling representation. Significantly, in this model Y685, the residue predominantly phosphorylated following VEGF stimulation (Wallez et al., 2006), is not accessible when β-catenin is bound.

Europe PMC Funders Author Manuscripts

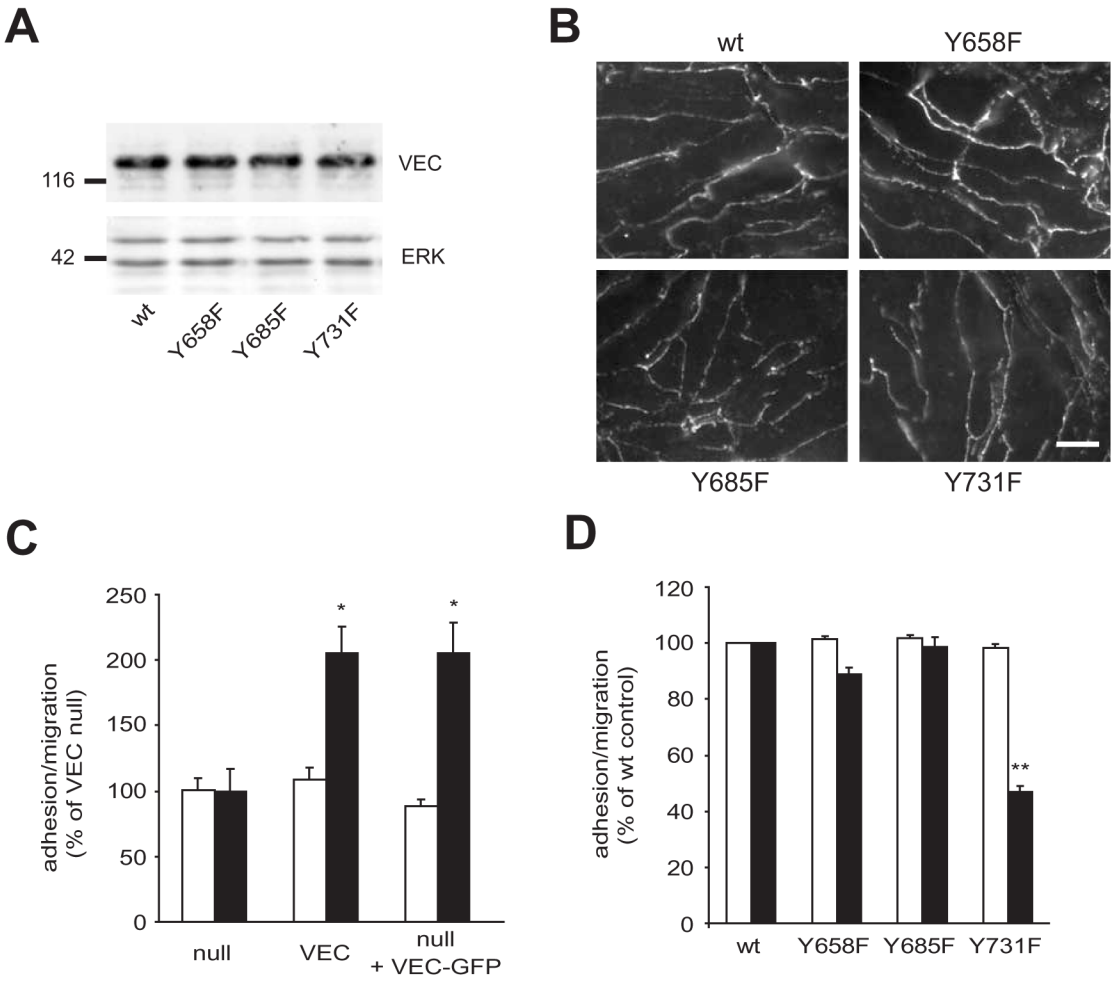

Fig. 4.

Y731 within the intracellular domain of VEC is important for lymphocyte migration. Mouse endothelioma cell lines, null for VEC and stably re-expressing wt or Y to F mutants of VEC were grown to confluence. (A) Equal amounts of proteins were analysed by immunoblotting using anti-VEC and anti-ERK antibodies. The position of size markers (in kDa) is indicated on the left. (B) Immunocytochemical analysis of the VEC distribution. Bar, 10 μm. (C) Mouse endothelioma cell lines, null for VEC, stably re-expressing wt VEC or transiently nucleofected with VEC-GFP were grown to confluence. They were then incubated with antigen-specific T cells, which were allowed to adhere and migrate for 4 hours. Adhesion (white) and migration (black) across these EC populations was then determined as described in the Methods section. Results are expressed as % increase of VEC-null EC (mean ± SEM of six replicates from five independent experiments). (D) Lymphocyte migration across the indicated, stable mouse endothelioma cell lines. Adhesion (white) and migration (black) across individual transfected EC populations was then measured as above. Results are expressed as % of control cells re-expressing wt VEC (mean ± SEM of six replicates from at least three independent experiments). Significant differences were determined by Student's *t* test, * $p<0.005$, ** $p<0.0001$.

Europe PMC Funders Author Manuscripts

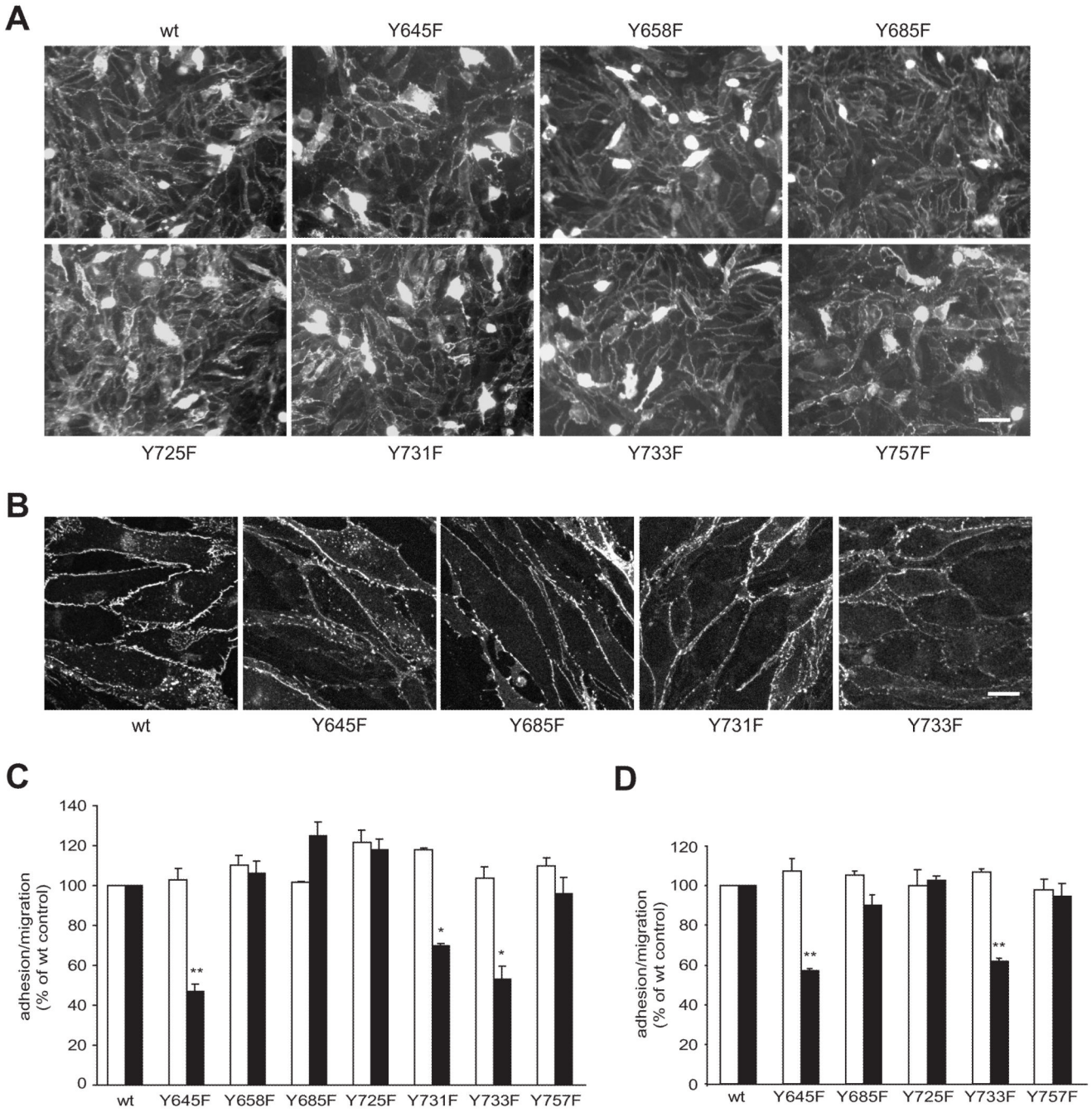

Fig. 5.

Y to F substitutions in the intracellular domain of VEC at positions 645, 731 or 733 affect lymphocyte migration in a dominant manner. GPNT brain microvascular EC were nucleofected with wt or Y to F mutants of pEGFP-N'-VEC. On average 80 % of cells expressed VEC-EGFP over a period of up to three to four days. (A) Shown here transfected GPNT cells that were fixed after 2 days and VEC-GFP distribution analyzed by fluorescent microscopy. Bar, 50 μm. (B) Three days after transfection, GPNT cells were fixed and VEC-GFP expression analysed by confocal microscopy. Bar, 10 μm. (C) Nulceofected GPNT were grown to confluence for 24-48 hours at which point equal expression was verified by fluorescent microscopy (see panel A). Lymphocyte adhesion (white) and

migration (black) was then measured as described in Fig. 4. (D) Mouse VEC-null endothelioma cells (see Fig. 4) were nucleofected with wt or the indicated Y to F mutants of pEGFP-N'-VEC before T cell adhesion and migration was assessed. Significant differences were determined by Student's *t* test, * $p<0.005$; ** $p<0.0001$.

Europe PMC Funders Author Manuscripts

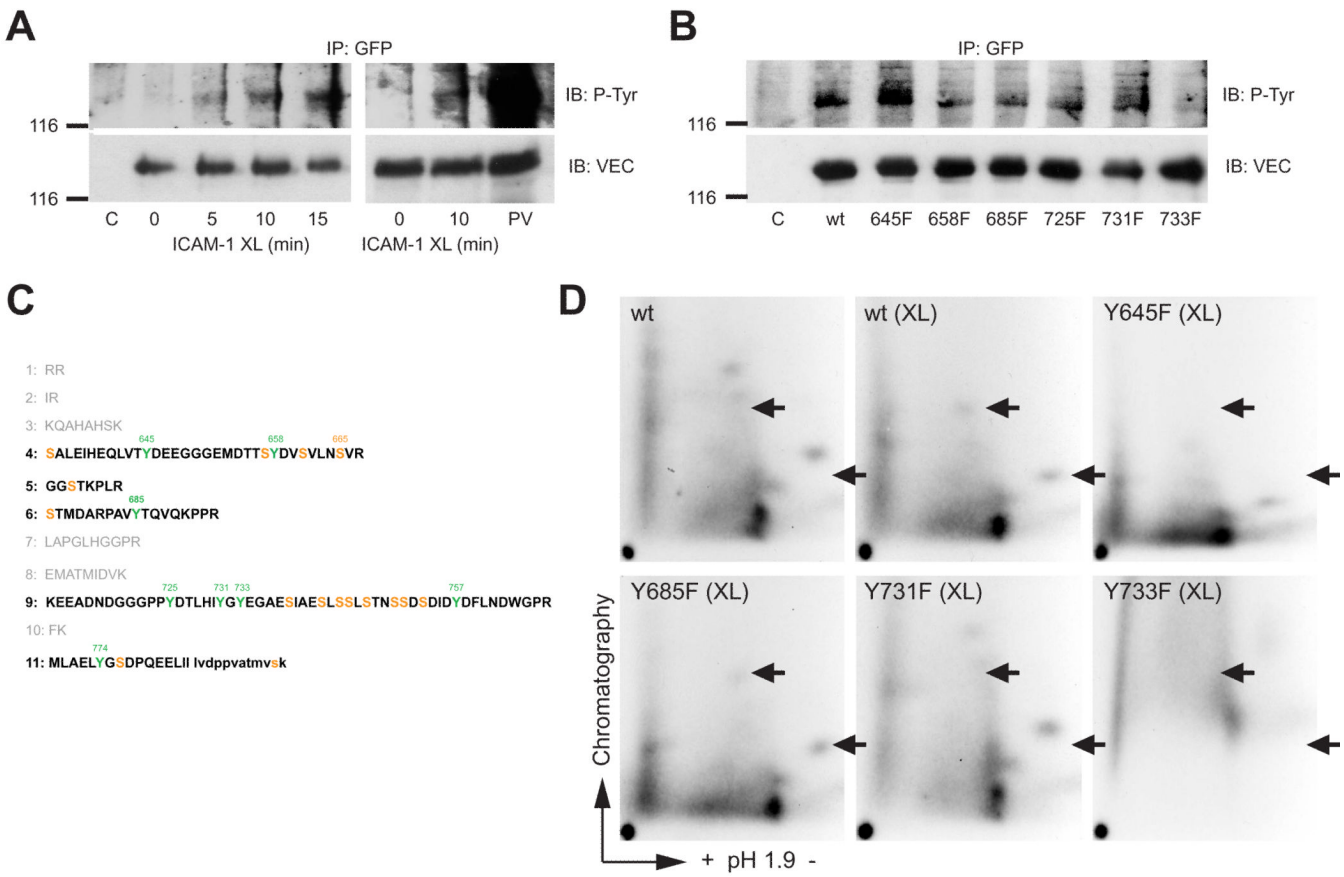

Fig. 6.

ICAM-1 induced VEC phosphorylation in wt and mutant VEC. (A) CHO-ICAM-1 cells were transfected with wt pEGFP-N'-VEC or not, grown to post-confluence and then starved. Cells were then subjected to ICAM-1 crosslinking and VEC-GFP immunoprecipitated and analysed by immunoblotting for phospho-tyrosine and VEC. C: untransfected controls, PV: sample from pervandate (100 μM) pretreated cells. (B) As described for panel A, except that the CHO-ICAM-1 cells were transfected with wt or Y to F mutants of VEC as indicated. ICAM-1 crosslinking was 10 minutes. (C) The sequence of the cytoplasmic domain of mouse VEC as shown in Fig. 3 A has been used to predict tryptic peptides. Amino acids in small letters in peptide 11 are from the linker sequence to EGFP (which is not shown). Five out of the eleven peptides (shown in bold) contain many phosphorylatable serine and tyrosine residues in line with our observation that VEC is strongly phosphorylated on serine and less so on tyrosine (data not shown). Note: in contrast to the report by Wallez et al. (2006) we have assumed that trypsin digestion does not occur when a proline is found at the carboxylic side of lysine or arginine. (D) CHO-ICAM-1 cells were transfected with pEGFP-N'-VEC as described above. Cells were labeled with 32P and then subjected to ICAM-1 crosslinking or not. VEC-GFP was immunoprecipitated and processed for tryptic peptide mapping. Arrowheads denote the position of crosslinking-specific phosphopeptides. The three maps displayed in a single row were chromatographed in the same tank and Rf values were directly comparable. Enlarged sections of the phospho-peptide maps showing ICAM-1 crosslinking specific phospho-peptides are shown in Supplemental Fig. S2.

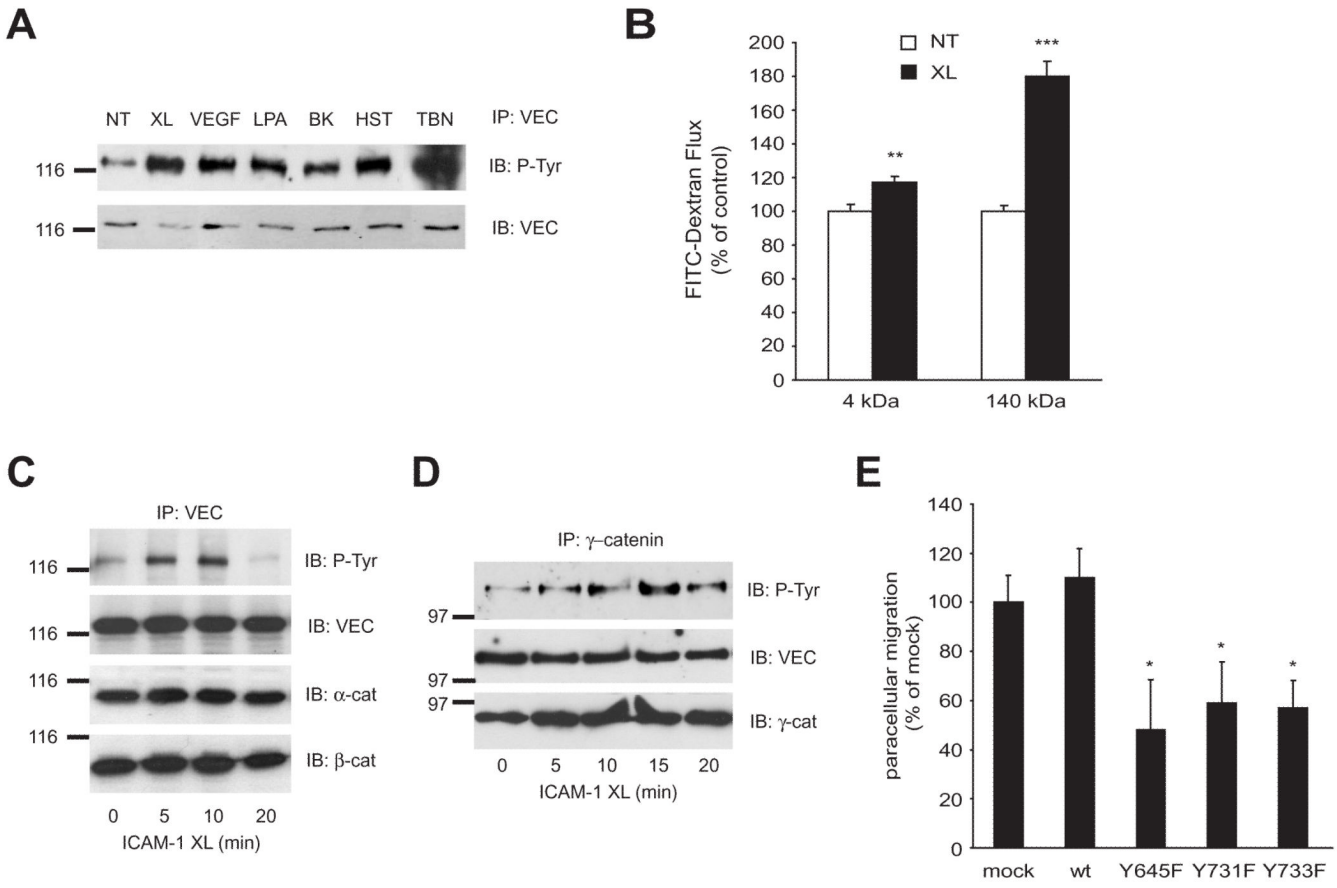

Fig. 7.

ICAM-1 mediated VEC phosphorylation affects paracellular migration and coincides with increased EC permeability. (A) GPNT brain microvascular ECs were grown to confluence, serum starved and then either left untreated (NT) or subjected to ICAM-1 crosslinking (XL), 50 ng/mL VEGF, 10 mM lysophosphatidic acid (LPA), 10 μM bradykinin (BK), 100 μM histamine (HST) or 1U/mL thrombin (TBN) for 15 minutes. Subsequently, cells were lysed and VEC immunoprecipitates analysed by immunoblots using anti-phospho-tyrosine or –VEC antibodies. (B) The flux of 4 or 140 kDa FITC-dextran across confluent GPNT monolayers was measured when ICAM-1 was crosslinked (XL) or not (NT). In each case, the FITC-dextran flux was linear over 120 minutes. The values shown are mean permeability changes that occurred over the initial linear 50-minute period following crosslinking in three independent experiments. (C, D) Confluent GPNT EC were serum starved and ICAM-1 crosslinked (XL). At the indicated times cells were lysed and subjected to immunoprecipitation of VEC (C) or γ-catenin (D). Immunoprecipitates were then analysed by immunoblotting using antibodies against phospho-tyrosine, α-, β-, γ-catenins or VEC. Similar results were achieved when the order of the proteins for immunoprecipitates and immunoblots was inverted (Fig. 2 and data not shown). In all blots the position of size markers (in kDa) is indicated on the left. (E) GPNT brain microvascular EC were nucleofected with wt or Y to F mutants of pEGFP-N'-VEC as described in Figure 3. They were then incubated with antigen-specific T cells, which were allowed to adhere and migrate for 1-4 h. Subsequently time-lapsed microscopy was performed over a 5 to 10 minutes to determine the fraction of T cells migrating in the paracellular area of the EC. Results are the mean ± SEM of six replicates from at least three independent experiments. Significant differences were determined by Student's *t* test, * $p<0.05$, ** $p=0.005$, *** $p<0.0001$.